Eur. Phys. J. B **3**, 257–261 (1998)

THE EUROPEAN PHYSICAL JOURNAL B

Resonance splitting effect in semiconductor superlattices

Y. Guo[1,3,a], B.-L. Gu[1,2], Z.-Q. Li[3], Q. Sun[3], and Y. Kawazoe[3]

[1] Department of Physics, Tsinghua University, Beijing 100084, P.R. China
[2] Center for Advanced Study, Tsinghua University, Beijing 100084, P.R. China
[3] Institute for Materials Research, Tohoku University, Sendai 980-8577, Japan

Received: 12 October 1997/ Revised and Accepted: 5 January 1998

Abstract. The resonance splitting in finite semiconductor superlattices which consist of a number of electric barriers is investigated. It is found that $(n-1)$-fold splitting for n-barrier tunneling obtained in periodic superlattices of identical barriers no longer holds for superlattices which are periodically juxtaposed with two different building barriers. In general, one resonant domain in the former splits into two resonant subdomains in the latter, and splitting occurs each time when two new barriers are added. The results indicate that the resonance splitting is determined not only by the structure but also by the parameters of building blocks.

PACS. 73.40.Gk Tunneling – 73.40.Kp III-V semiconductor-to-semiconductor contact, p-n junctions, and heterojunctions

1 Introduction

Since the pioneering work done by Tsu and Esaki [1] there has been a lot of research work on electronic transport properties in semiconductor superlattices, especially tunneling phenomena [2–11]. It is understood that it is the resonant-tunneling process that leads to the negative differential conductance. An interesting feature emerged from the studies on multibarrier tunneling is that the resonance in transmission exhibits some splitting effects. Based on finite superlattices with periodic potential structure, Tsu and Esaki [1] first pointed out that for n-barrier tunneling the splitting would be $(n-1)$-fold. Furthermore, they remarked that the split resonance energies would eventually approach the band model results for very large n. Vassell, Lee, and Lockwood [2] developed a general theory of multibarrier tunneling, which did not deal with the resonance splitting effect. Experimental investigation on the superlattice miniband position by means of hot-electron injection was reported by Kuan, Tsui, and Choi [3], in which the bias across the superlattice is always kept at zero. Most recently, $(n-1)$-fold splitting for n-barrier tunneling was proved analytically by Liu and Stamp [9,10] in the semiconductor superlattice which are modeled by periodically arranging identical potential barriers and wells with arbitrary profiles at zero bias.

However, there are still some basic questions unclear. For example, what happens for resonance splitting in superlattices which are periodically arranged with two different building barriers? Does $(n-1)$-fold splitting for n-barrier tunneling still hold for this case? In this paper, we have confirmed that features of splitting strongly depend not only on the structure but also on the parameters of building barriers. We also make some discussion on transition between complete and incomplete transmission resonances, and transition between singlet and doublet resonances in triple-barrier structures, which are helpful to understand resonance splitting features exhibited in finite semiconductor superlattices.

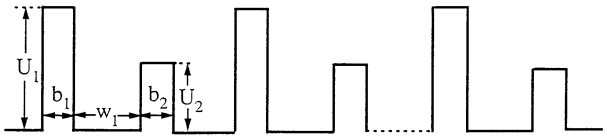

Fig. 1. A semiconductor superlattice is periodically arranged with two different building barriers. U_1 and U_2 are the heights of adjacent barriers, b_1 and b_2 are the widths of them, w_1 is the width of the first well, respectively.

2 Method

Consider electrons tunneling through a finite $GaAs/Ga_{1-x}Al_xAs$ (x is Al-concentration in the $Ga_{1-x}Al_xAs$ barrier regions) semiconductor superlattice along the z direction as depicted in Figure 1, where U_1 and U_2 are heights of two adjacent building barriers, b_1 and b_2 are widths of them, respectively; w_1 is the width of the first quantum well. One-dimensional Schrödinger equation in the framework of the effective

[a] e-mail: guoy@phys.tsinghua.edu.cn

mass approximation is as follows,

$$\left[\frac{1}{2m^*}\frac{d^2}{dz^2}+U(z)\right]\Psi(z)=E\Psi(z), \tag{1}$$

where $U(z)$ is the potential of the semiconductor superlattice, E is the incident energy of an electron, and m^* is the effective mass of the incident electron.

In the incident and outgoing regions, the wave functions of the particle are plane waves

$$\Psi(z)=\begin{cases}\exp(ik_z z)+r\exp(-ik_z z),\\ \tau\exp(ik_z z),\end{cases} \tag{2}$$

where $k_z = (2m_0^* E)^{1/2}/\hbar$, $\hbar(= h/2\pi)$ is the reduced Planck constant, and m_0^* is the effective mass of electron at the incident (outgoing) regions, which is taken to be $0.067m_e$ for GaAs case (m_e is the free electron mass). r and τ are the reflection and transmission amplitudes, respectively.

In the jth barrier region, the wave functions can readily be expressed in terms of exponential functions (for $E < U_j$) or expressed by plane waves (for $E > U_j$)

$$\Psi_b^j(z)=\begin{cases}A_b^j\exp(\kappa_b^j z)+B_b^j\exp(-\kappa_b^j z), & E<U_j,\\ A_b^j\exp(ik_b^j z)+B_b^j\exp(-ik_b^j z), & E>U_j,\end{cases} \tag{3}$$

where $\kappa_b^j = [2m_b^j(U_j-E)]^{1/2}/\hbar$, $k_b^j = [2m_b^j(E-U_j)]^{1/2}/\hbar$, and U_j is the height of the jth barrier.

In the jth well region, the wave functions are still plane wave functions

$$\Psi_w^j(z)=A_w^j\exp(ik_w^j z)+B_w^j\exp(-ik_w^j z), \tag{4}$$

where $k_w^j = [2m_w^j E]^{1/2}/\hbar$.

To meet current flux density conservation, the boundary conditions (*i.e.* continuity of the wave function Ψ and its appropriately normalized derivative $(1/m^*)(d\Psi/dz)$ at the boundaries) are required. This leads to the following relationship between the reflection amplitude r and transmission amplitude τ

$$\begin{bmatrix}1\\ r\end{bmatrix}=\frac{1}{2ik_z}\begin{bmatrix}ik_z & 1\\ ik_z & -1\end{bmatrix}S(z)\times\begin{bmatrix}1 & 1\\ (m_b^n/m_0^*)ik_z & -(m_b^n/m_0^*)ik_z\end{bmatrix}\begin{bmatrix}\tau\\ 0\end{bmatrix}, \tag{5}$$

where

$$S(z)=S_b^1(b_1)S_w^1(w_1)S_b^2(b_2)S_w^2(w_2)\ldots S_b^n(b_n), \tag{6}$$

b_j and w_j are the widths of the jth barrier and jth well, respectively; S_b^j and S_w^j correspond to the transfer matrices for the jth barrier and jth well, respectively:

$$S_b^j(b_j)=\begin{pmatrix}\cosh(\kappa_b^j b_j) & -\frac{1}{\kappa_b^j}\sinh(\kappa_b^j b_j)\\ -\frac{m_w^{j-1}}{m_b^j}\kappa_b^j\sinh(\kappa_b^j b_j) & \frac{m_w^{j-1}}{m_b^j}\kappa_b^j\cosh(\kappa_b^j b_j)\end{pmatrix}\quad(E<U_j) \tag{7}$$

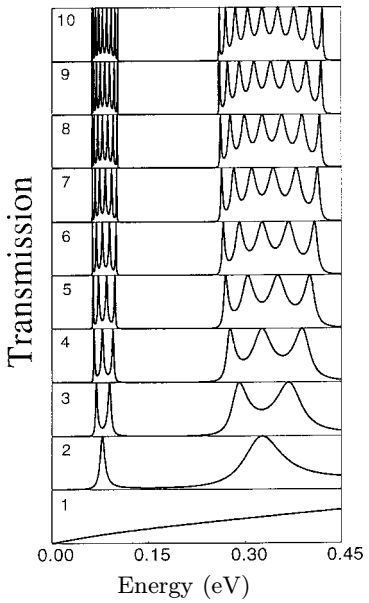

Fig. 2. Transmission *versus* energy for electrons tunneling through from a single barrier ($n = 1$) to a finite superlattice of ten identical barriers. The numbers indicated in each subplot denote the total number of barriers in the corresponding structure. $U_j = 300$ meV, $b_j = 20$ Å, $w_j = 50$ Å, $m_b^j = 0.1002m_e$, $m_w^j = 0.067m_e$, $j = 1, 2, \cdots$.

$$S_b^j(b_j)=\begin{pmatrix}\cos(k_b^j b_j) & -\frac{1}{k_b^j}\sin(k_b^j b_j)\\ \frac{m_w^{j-1}}{m_b^j}k_b^j\sin(k_b^j b_j) & \frac{m_w^{j-1}}{m_b^j}k_b^j\cos(k_b^j b_j)\end{pmatrix}\quad(E>U_j) \tag{8}$$

$$S_w^j(w_j)=\begin{pmatrix}\cos(k_w^j w_j) & -\frac{1}{k_w^j}\sin(k_w^j w_j)\\ \frac{m_b^j}{m_w^j}k_w^j\sin(k_w^j w_j) & \frac{m_b^j}{m_w^j}k_w^j\cos(k_w^j w_j)\end{pmatrix}. \tag{9}$$

Therefore, the transmission coefficient T for electrons tunneling through an n-barrier superlattice is given by

$$T(E)=4[(S_{11}+\frac{m_b^n}{m_0^*}S_{22})^2+(\frac{S_{21}}{k_z}-\frac{m_b^n}{m_0^*}k_z S_{12})^2]^{-1}, \tag{10}$$

where S_{11}, S_{12}, S_{21}, and S_{22} are the elements of the $S(z)$ matrix.

3 Numerical results and discussion

Figure 2 presents the transmission coefficient as the function of the incident energy for electrons tunneling through from a single barrier to finite periodic superlattices. The barriers in the superlattices are identical ($U_j = 300$ meV and $b_j = 20$ Å). Throughout this paper we have set $m_b^j = 0.1002m_e$ for barriers with height $U_j = 300$ meV, $m_b^j = 0.0836m_e$ for barriers with height $U_j = 150$ meV, $w_j = 50$ Å and $m_w^j = 0.067m_e$ for all wells. The barrier

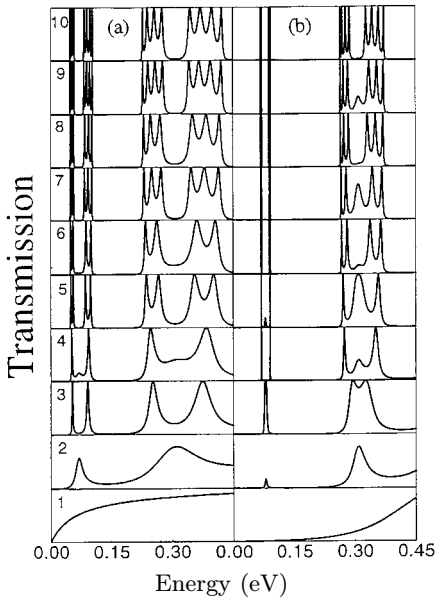

Fig. 3. Transmission *versus* energy for electrons tunneling through from single barriers ($n = 1$) to finite superlattices which are periodically arranged with two different building barriers. (a) $U_1 = 150$ meV, $b_1 = 20$ Å (for $n = 1$); $U_{2j-1} = 300$ meV, $U_{2j} = 150$ meV, $b_j = 20$ Å, $w_j = 50$ Å, $m_b^{2j-1} = 0.1002m_e$, $m_b^{2j} = 0.0836m_e$, $m_w^j = 0.067m_e$, $j = 1, 2, \cdots$ (for $n \geq 2$). (b) $U_1 = 300$ meV, $b_1 = 40$ Å (for $n = 1$); $U_j = 300$ meV, $b_{2j-1} = 20$ Å, $b_{2j} = 40$ Å, $w_j = 50$ Å, $m_b^j = 0.1002m_e$, $m_w^j = 0.067m_e$, $j = 1, 2, \cdots$ (for $n \geq 2$).

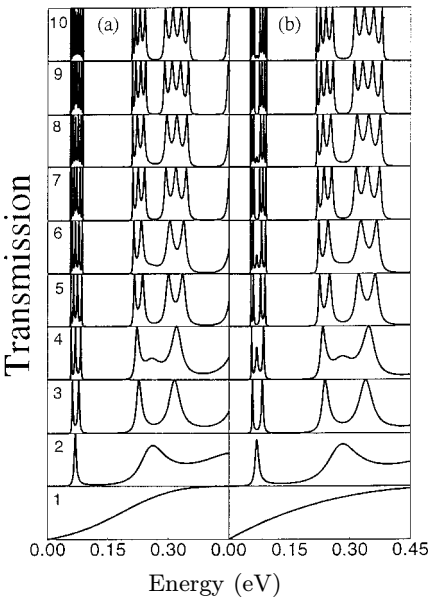

Fig. 4. Transmission *versus* energy for electrons tunneling through from single barriers ($n = 1$) to finite superlattices which are periodically arranged with two different building barriers. (a) $U_1 = 150$ meV, $b_1 = 40$ Å (for $n = 1$); $U_{2j-1} = 300$ meV, $U_{2j} = 150$ meV, $b_{2j-1} = 20$ Å, $b_{2j} = 40$ Å, $w_j = 50$ Å, $m_b^{2j-1} = 0.1002m_e$, $m_b^{2j} = 0.0836m_e$, $m_w^j = 0.067m_e$, $j = 1, 2, \cdots$ (for $n \geq 2$). (b) $U_1 = 150$ meV, $b_1 = 30$ Å (for $n = 1$); $U_{2j-1} = 300$ meV, $U_{2j} = 150$ meV, $b_{2j-1} = 20$ Å, $b_{2j} = 30$ Å, $w_j = 50$ Å, $m_b^{2j-1} = 0.1002m_e$, $m_b^{2j} = 0.0836m_e$, $m_w^j = 0.067m_e$, $j = 1, 2, \cdots$ (for $n \geq 2$).

height and the effective mass of electrons are determined by the Al-concentration x in the $Ga_{1-x}Al_xAs$ barrier regions [12]. The range of the transmission coefficient is from 0 to 1 in each subplot of Figure 2. It is evident from Figure 2 that there is no resonance peak for the single barrier in the considered energy region. Resonance peaks begin to appear from $n = 2$, and each time when a new barrier is added to the existing ones, the resonance splitting occurs. For n-barrier tunneling, the splitting is $(n-1)$-fold. The results obtained here once again prove the generalization of Tsu *et al.* [1] and Liu *et al.* [9,10]. One can also see that with increasing the number of barriers in the superlattice, resonant domains are broadened and located almost at the center of peaks of the double-barrier structure.

The case what we are most interested in is that superlattices which are periodically juxtaposed with two different building barriers. Figures 3a and 3b show the transmission coefficient as the function of the incident energy for electrons tunneling through from a single barrier to finite superlattices, in which two different barriers are periodically arranged. Here two single barriers are chosen to be different from that in Figure 2. The range of the transmission coefficient for each subplot is from 0 to 1. Figure 3a presents the results for the superlattices where building barriers have different heights ($U_{2j-1} = 300$ meV, $U_{2j} = 150$ meV, $j = 1, 2, \cdots$), whereas the barrier width and well width are set to be $b_j = 20$ Å and $w_j = 50$ Å, respectively. Figure 3b shows the results for the superlattices in which building barriers have different widths ($b_{2j-1} = 20$ Å, $b_{2j} = 40$ Å, $j = 1, 2, \cdots$) whereas the barrier height and the well width are set to be $U_j = 300$ meV and $w_j = 50$ Å, respectively. Comparing Figure 3 with Figure 2, it is evident that one resonant domain in the periodic superlattice which consists of identical barriers splits into two resonant subdomains in the superlattice which is periodically juxtaposed with two different barriers. In each resonant subdomain there is smaller number of resonance peaks. The total number of peaks is not always equal to $(n-1)$ for n-barrier tunneling. Moreover, the resonance splitting occurs each time when two new barriers are added to the existing ones. Here we would like to point out that the total number of resonance peaks in each resonant subdomain in the low energy region is exactly same as that in the high energy region. In our plots some peaks in the low energy region are too close to discern clearly. In addition, although to some extent the feature of the resonance splitting displayed in Figures 3a and 3b is similar, there still exist some discrepancies between these two cases. The most obvious discrepancy is that in the superlattices where two building barriers have different widths and same heights, resonance peaks becomes sharper and the width of each resonant subdomain is dramatically narrowed, especially in the low incident energy region due to larger width of the whole structure.

In Figure 3 the two building barriers have different widths and same heights or have different heights and same widths. For a general case, *i.e.*, two building barriers are different from each other on both width and height, do the above stated splitting features still exist? Figures 4a and 4b show the transmission coefficient as the function of the incident energy for electrons tunneling through from single barrier structures to finite superlattices. The parameters of barriers in Figure 4a are set to be $b_{2j-1} = 20$ Å, $U_{2j-1} = 300$ meV, $b_{2j} = 40$ Å, and $U_{2j} = 150$ meV ($j = 1, 2, \cdots$). In this case, we carefully choose barrier width and height in order to obtain unity peak-value for first resonance peak in the double-barrier structure. The parameters of barriers in Figure 4b are chosen to be $b_{2j-1} = 20$ Å, $U_{2j-1} = 300$ meV, $b_{2j} = 30$ Å, $U_{2j} = 150$ meV ($j = 1, 2, \cdots$). From Figure 4a one can see that for first resonant domain, the resonance splitting resembles to that of superlattices of identical building barriers, *i.e.*, $(n-1)$-fold splitting for n-barrier tunneling. A noticeable result is that for the structures with even number of building blocks, the middle peak in the low energy region is less than unity ($n = 6$, 8, 10). However, for the second larger resonant domain in the high incident energy, splitting features resemble to those exhibited in Figure 3 where the structures are obtained by periodically arranging two different barriers. For superlattices of arbitrary building barriers shown in Figure 4b, one can see that the splitting features resemble to those displayed in Figure 3.

How can we understand these interesting resonance splitting features displayed in periodic superlattices? The resonance splitting is driven by its energy-band structure of the corresponding superlattice, which is determined not only by the structure but also by the parameters of building barriers. As we know, eigenlevels of the independent quantum wells are split due to the coupling between the wells via tunneling through the barriers. Consequently, these split levels redistribute themselves in groups around their unperturbed positions and form quasibands. As the number of periods tends to infinity, the energy band is formed. For a finite superlattice, there is no continuous energy band. In each band, only some discrete energy could be expected. Moreover, one band which consists of several separated quasibound energy levels in the superlattice of identical barriers splits into two subbands in the superlattice arranged with two different barrier. Each subband includes smaller number of quasibound energy levels. The necessary condition for the resonant tunneling to occur is that the energy of the incident energy falls completely inside the allowed bands. Therefore, in the transmission spectrum one can naturally see above stated resonance splitting. The positions of the resonance peaks predict the quasibound energy levels of the interacting multiwell structures.

Finally, we make some discussion on two interesting types of resonance transitions existed in triple-barrier structures, which are helpful to further understand resonance splitting features shown in Figures 2 to 4. First of all, an important fact to note is that the physics of resonant tunneling in the triple-barrier structure is much more than an extension of the results of the double barrier case, since the former involves the coupling of quasibound states between two adjacent quantum wells. From Figures 3 and 4 it is evident that there exists a transition of transmission resonances for electrons tunneling through from simple asymmetric double-barrier structure to comparatively complex structures of unidentical barriers, such as triple-barrier structures. Complete resonant tunneling can occur in the latter case as in structures of identical barriers. However, in the triple-barrier case, if the difference between adjacent barriers is further enlarged, one can still see the reduction of transmission peaks.

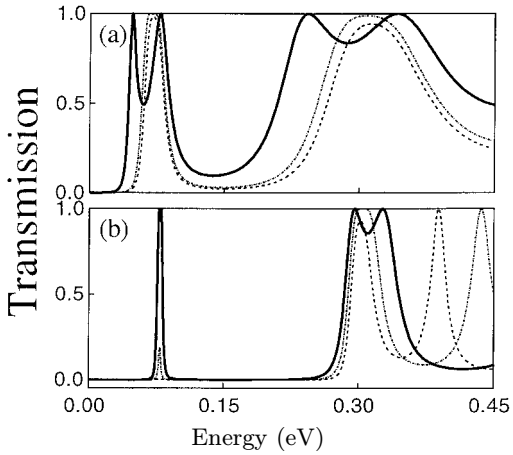

Fig. 5. Transmission *versus* energy for electrons tunneling through triple-barrier structures. $w_1 = w_2 = 50$ Å. In all of plots, $m_b^j = 0.0836m_e, 0.1002m_e, 0.10345m_e$ correspond to barriers with height $U_j = 150$ meV, 300 meV, 337.5 meV, respectively. (a) $b_1 = b_2 = b_3 = 20$ Å, $U_1 = U_3 = 150$ meV. The solid, dot-dashed, and dashed lines correspond to $U_2 = 150$ meV, 300 meV, 337.5 meV, respectively. (b) $U_1 = U_2 = U_3 = 300$ meV, $b_1 = b_3 = 20$ Å. The solid, dot-dashed, and dashed lines correspond to $b_2 = 40$ Å, 60 Å, 80 Å, respectively.

Figure 5a shows the numerical results of the transmission coefficient *versus* incident energy for electrons tunneling through three triple-barrier structures. The height of the middle barrier is different whereas the widths of three barriers are set to be same and equal to 20Å. The solid, dot-dashed, and dashed lines correspond to $U_2 = 150$ meV, 300 meV, 337.5 meV, respectively. Other parameters are chosen to be $U_1 = U_3 = 150$ meV. Figure 5b displays the results for electrons tunneling through three triple-barrier structures in which the middle barrier with different widths, whereas the width of left barrier and that of the right one are set to be same and equal to 20 Å. The barrier height is chosen to be same as ($U_1 = U_2 = U_3 = 300$ meV). The solid, dot-dashed, and dashed lines correspond to the cases with $b_2 = 40$ Å, 60 Å, 80 Å, respectively. There are two distinct features which should be noticed. One is that resonance peaks drop off with enlarging the difference between the middle barrier and side ones, especially for the cases in Figure 5b where the first peak drop drastically (see the dashed line). It is too low to see clearly. Here we would like to point out that in Figure 5b two resonance peaks in the low incident

energy region (see the solid line) is too close to discern. If we enlarge them, two separated resonant peaks can be clearly seen. In the triple-barrier case of unidentical barriers, whether complete resonant tunneling can occur or not strongly depends on the degrees of discrepancy between adjacent barriers. This is one type of transitions between complete and incomplete transmission resonances existed in triple-barrier structures. The other is that there exists transitions between doublet resonances (*i.e.*, tunneling with doublet) and singlet resonances (*i.e.*, tunneling with singlet). When enlarging the difference between building blocks in the triple-barrier case, tunneling with doublet turns into tunneling with singlet. The origin of the existence of these two types of resonance transitions is due to the complex coupling between two quantum wells within barriers.

4 Conclusions

The resonance splitting in semiconductor superlattices are determined not only by the structure but also by the parameters of building barriers. The mechanism of splitting is driven by its energy-band structure of the corresponding superlattice. Two kinds of periodic superlattices are examined. One is a periodic arrangement with identical barriers while the other is periodically juxtaposed with two different building barriers. In general, one resonant domain in the former splits into two resonant subdomains in the latter. For n-barrier tunneling, splitting is not always $(n-1)$-fold. There exist two interesting and complex types of resonance transitions which are helpful to understand tunneling properties in multibarrier structures. One is between complete and incomplete transmission resonances. The other is between singlet and doublet resonances.

Two of us (Yong Guo and Bing-Lin Gu) would like to acknowledge partial support from the High Technology Research and Development Program of P. R. China.

References

1. L. Esaki, R. Tsu, IBM J. Rev. Dev. **14**, 61 (1970); R. Tsu, L. Esaki, Appl. Phys. Lett. **22**, 562 (1973).
2. M.O. Vassell, J. Lee, H.F. Lockwood, J. Appl. Phys. **54**, 5206 (1983).
3. C.H. Kuan, D.C. Tsui, K.K. Choi, Appl. Phys. Lett. **61**, 456 (1992).
4. B. Ricco, M.Y. Azbel, Phys. Rev. B **29**, 1970 (1984).
5. E.E. Mendez, in *Physics and Applications of Quantum wells and Superlattices*, edited by E.E. Mendez and K. von Klitzing (Plenum, New York, 1987).
6. S.S. Allen, S.L. Richardson, Phys. Rev. B **50**, 11693 (1994).
7. X.D. Zhao, H. Yamamoto, Z.M. Chen, K. Taniguchi, J. Appl. Phys. **79**, 6966 (1996).
8. Y. Guo, B.L. Gu, W.H. Duan, Z. Phys. B **102**, 217 (1997).
9. X.W. Liu, A.P. Stamp, Phys. Rev. B **47**, 16605 (1993).
10. X.W. Liu, A.P. Stamp, Phys. Rev. B **50**, 1588 (1994).
11. X.H. Wang, B.Y. Gu, G.Z. Yang, Phys. Rev. B **55**, 9340 (1997).
12. H.C. Casey, M.B. Panich, *Heterostructure Lasers* (Academic, New York, 1978), Pt. A, Chap. 4.